DALTON
FULL PAPER

The influence of the linkage mode between bipyridine units in oligobipyridine ligands on the formation of copper-(I) and -(II) helicates

Mou-Hai Shu,[a] Wei-Yin Sun,*[a] Chun-Ying Duan,[a] You-Jun Fu,[a] Wen-Jian Zhang[b] and Wen-Xia Tang*[a]

[a] *State Key Laboratory of Coordination Chemistry, Coordination Chemistry Institute, Nanjing University, Nanjing 210093, China*

[b] *State Key Laboratory of Structural Chemistry, Fujian Institute of Research on the Structure of Matter, Chinese Academy of Sciences, Fuzhou 350002, China*

Received 3rd November 1998, Accepted 24th December 1998

A novel asymmetric oligobipyridine ligand, 1-(5′-methyl-2,2′-bipyridin-5-yl)-2-(6′-methyl-2,2′-bipyridin-6-yl)ethane (L^{56}), was synthesized, and double-stranded helical complexes $[Cu^{I}_2L^{56}_2][ClO_4]_2\cdot Et_2O$ **1** and $[Cu^{II}_2L^{56}_2(OH)(H_2O)][ClO_4]_3$ **2** were obtained by reaction of the ligand with copper-(I) and -(II) ions, respectively. X-Ray data for **1** show that the two ligands intertwine around the two copper(I) ions with distorted tetrahedral geometry. The distance between the two Cu(I) ions is 7.290(2) Å. The copper(II) ions in **2** have a disordered tetragonal pyramidal geometry with a N_4O donor set. The intermetallic distance is 6.875(2) Å. In both **1** and **2** the two ligand strands are arranged in a head-to-tail configuration. The complexes were also characterized by ES-MS, ^1H NMR and ESR spectroscopies. The results show that the difference in linkage of the spacer group to the bipyridine units produces a great impact on the helix formation with Cu^{II}.

Introduction

There is current interest in inorganic helical complexes containing metal ions.[1–4] Double[3,5–8] and triple[9,10] helical structures have been generated by complexation of ligands with two or more metal ions. In these supramolecular constructions the formation of the helicates can be described as the result of reading molecular information stored in the ligands by metal ions following the co-ordination algorithm such as tetrahedral and octahedral *etc.*[9] The type of structure is determined by the nature and arrangement of the binding subunits in the strands, and the co-ordination geometry of the metal ions which determine the steric program and the reading algorithm of the self-assembly process. Previous works have shown that oligobipyridine ligands containing bipyridine units linked by CH_2OCH_2 or CH_2CH_2 group at the 6,6′ positions co-ordinate to silver(I)[7] and copper(I)[3,5] with tetrahedral co-ordination geometry to form double helicates, but cannot form a double helix with Cu^{II}. On the other hand, such units linked at the 5,5′ positions co-ordinate to nickel(II) and iron(II) with octahedral co-ordination geometry to give a triple helicate[3,9] and circular tetranuclear,[11] pentanuclear[12] and hexanuclear[11] double helices. It seems that the self-assembly process of supramolecular helicates is not only controlled by the co-ordination geometry of metal ions and the flexibility of the spacer groups in the ligands, but also influenced by the linkage mode of the spacer group to the bipyridine units in the oligobipyridine ligands. In order to illustrate the effect of the bridge between the bipyridine units in the oligobipyridines on the formation of inorganic helicates, we designed and synthesized a novel ligand L^{56}, in which two bipyridine units are connected by a CH_2CH_2 spacer group at the 5,6′ positions, and investigated the reaction of L^{56} with Cu^{I}, Cu^{II}, *etc.* The results show that L^{56} not only co-ordinated to copper(I) to form a double helical complex $[Cu^{I}_2L^{56}_2][ClO_4]_2\cdot Et_2O$ **1** which is similar to that obtained with the reported ligand L^{66},[3] but also co-ordinated to Cu^{II} giving a dinuclear double-stranded helical complex $[Cu^{II}_2L^{56}_2(OH)(H_2O)][ClO_4]_3$ **2**, a species which has not been obtained using the reported ligands L^{55} and L^{66}.[3,9]

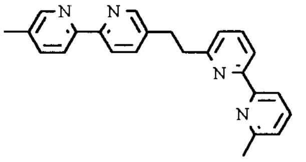

L^{56}

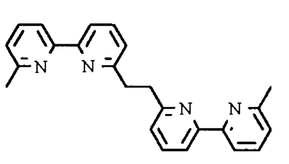

L^{66}

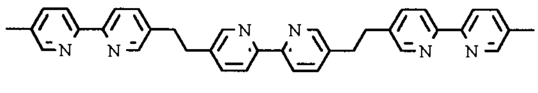

L^{55}

Experimental

Materials

Tetrahydrofuran (THF) was dried by sodium with benzophenone and distilled before use. Acetonitrile was purified by treatment with $KMnO_4$ and then distilled over P_2O_5 and K_2CO_3. 6-Hydroxymethyl-6′-methyl-2,2′-bipyridine,[13] 5,5′-dimethyl-2,2′-bipyridine[14] and $[Cu(CH_3CN)_4]ClO_4$[15] were synthesized according to literature methods. All other chemicals were of reagent grade quality obtained from commercial sources and used without further purification.

Preparations

6-Bromomethyl-6′-methyl-2,2′-bipyridine. This compound reported in the literature[16] was obtained as a by-product with poor yield. We prepared this compound by the method similar to that for synthesis of 6-chloromethyl-6′-methyl-2,2′-bipyridine.[13] A mixture of 6-hydroxymethyl-6′-methyl-2,2′-bipyridine (1.2 g, 6 mmol) and phosphorus tribromide (6 ml) was refluxed for 30 min and then concentrated in vacuum to afford a dark residue, which was hydrolysed slowly with care and neutralized with a saturated Na_2CO_3 solution to pH > 8.5. The crude product was obtained by filtration and chromatographed on a silica column with ethyl acetate–light petroleum, bp range 60–90 °C, (1 : 4) to give 1.3 g of the white powder product. Yield 81%, mp 88–89 °C (lit.[16] 88 °C). ^{1}H NMR ($CDCl_3$): δ 2.73 (s, 3 H), 4.73 (s, 2 H), 7.26 (d, 1 H), 7.54 (d, 1 H), 7.79 (t, 1 H), 7.90 (t, 1 H), 8.34 (d, 1 H) and 8.44 (d, 1 H).

1-(5′-Methyl-2,2′-bipyridin-5-yl)-2-(6′-methyl-2,2′-bipyridin-6-yl)ethane (L^{56}). The ligand L^{56} was prepared under an argon atmosphere using standard Schlenk techniques. Diisopropylamine, butyllithium, 5,5′-dimethyl-2,2′-bipyridine, and 6-bromomethyl-6′-methyl-2,2′-bipyridine were used in anhydrous THF at −78 °C according to the procedures reported for preparing L^{55}.[9] The crude product was washed with methanol (10 ml) three times, chromatographed on a silica column with light petroleum (bp range: 60–90 °C)–acetone (5 : 1 v/v), and then recrystallized from acetonitrile, dried in vacuum, yield *ca.* 60%, mp 140–142 °C. ES-MS: *m*/*z* 367.1 (LH^+). ^{1}H NMR (CD_3CN at 298 K): δ 2.37 (s, 3 H), 2.58 (s, 3 H), 3.22 (s, 4 H), 7.21 (d, 1 H), 7.24 (d, 1 H), 7.67 (dd, 1 H), 7.71 (dd, 1 H), 7.73 (t, 1 H), 7.76 (t, 1 H), 8.22 (d, 1 H), 8.23 (d, 1 H), 8.24 (d, 2 H), 8.26 (d, 1 H), 8.40 (d, 1 H) and 8.48 (d, 1 H) (Found: C, 79.01; H, 6.27; N, 15.05. Calc. for $C_{12}H_{11}N_2$: C, 78.66; H, 6.05; N, 15.29%).

$[Cu^I_2L^{56}_2][ClO_4]_2\cdot Et_2O$ 1. A mixture of $[Cu(CH_3CN)_4]ClO_4$ (27 mg, 0.082 mmol) and L^{56} (30 mg, 0.082 mmol) in methanol (10 ml) was refluxed under an argon atmosphere for 2 h. Brown precipitates were obtained when ether (50 ml) was added to the resulting clear orange solution, filtered off and washed with ether, yield 38 mg (82%) of complex **1**. Single crystals suitable for X-ray structural analysis were obtained by slow diffusion of ether into the methanol solution. ^{1}H NMR (CD_3CN at 298 K): δ 2.05 (s, 3 H), 2.44 (s, 3 H), 3.18 (br, 4 H), 7.52 (d, 1 H), 7.59 (d, 1 H), 7.74 (d, 1 H), 8.04 (d, 1 H), 8.12 (t, 1 H), 8.17 (d, 1 H), 8.19 (t, 1 H), 8.27 (s, 1 H), 8.29 (d, 1 H), 8.32 (d, 1 H), 8.34 (d, 1 H) and 8.61 (s, 1 H) (Found: C, 54.75; H, 4.68; N, 10.06. Calc. for $C_{52}H_{54}Cl_2Cu_2N_8O_9$: C, 55.12; H, 4.80; N, 9.89%).

$[Cu^{II}_2L^{56}_2(OH)(H_2O)][ClO_4]_3$ 2. The ligand L^{56} (60 mg, 0.164 mmol) was suspended in 10 ml of acetonitrile, and copper(II) acetate monohydrate (32.7 mg, 0.164 mmol) in water (3 ml) was added dropwise. After stirring for 2 h in an ice–water bath a clear blue solution was obtained. Several drops of saturated sodium perchlorate solution were added and the mixture was still clear. After keeping at 4 °C for 3 d blue crystals were obtained, yield 60 mg (69%) of complex **2**. Single crystals suitable for X-ray diffraction analysis were obtained by slow evaporation from the solution of acetonitrile and water at 4 °C (Found: C, 48.04; H, 4.12; N, 9.51. Calc. for $C_{48}H_{47}Cl_3Cu_2N_8O_{14}$: C, 48.31; H, 3.97; N, 9.39%).

CAUTION: perchlorate salts combined with organic ligands are potentially explosive and should be handled with care.

Crystallography

Parameters for data collection and refinement of complexes **1** and **2** are summarized in Table 1 and selected bond lengths and angles are listed in Table 2.

$[Cu^I_2L^{56}_2][ClO_4]_2\cdot Et_2O$ 1. The data were collected on a Siemens P4 four-circle diffractometer with graphite-monochromated Mo-Kα radiation ($\lambda = 0.71073$ Å) at 293(2) K using the θ–2θ scan mode with a variable scan speed 5.0–50.0° min^{-1} in ω. Data were corrected for Lorentz-polarization effects during data reduction using XSCANS,[17] and a semiempirical absorption correction from ψ scans was applied.

The structure was solved by direct methods and refined on F^2 by full-matrix least-squares methods using SHELXTL version 5.0.[18] One of the perchlorate anions is disordered. The site occupancy factors of these disordered oxygen atoms were refined as 0.46 for O(22), O(23) and O(24), 0.54 for O(22′), O(23′) and O(24′), respectively. All the non-hydrogen atoms were refined anisotropically. All the hydrogen atoms were placed in calculated positions (C–H 0.96 Å) assigned fixed isotropic thermal parameters at 1.2 times (1.5 times for CH_3 group) the equivalent isotropic U of the atoms to which they are attached and allowed to ride on their respective parent atoms. The contributions of these hydrogen atoms were included in the structure-factor calculations.

$[Cu^{II}_2L^{56}_2(OH)(H_2O)][ClO_4]_4$ 2. The measurement was performed on a Siemens SMART/CCD area detector diffractometer and 3-circle goniometer (fixed χ). Unit cell parameters were refined from the setting angles and observed ω angles of selected strong reflections taken from the complete data set. The structure was solved by direct methods, and full-matrix least-squares refinement was based on F^2 with all independent data. The positions of the metal atoms were obtained from an E-map. The other non-hydrogen atoms and the hydrogen atoms in the co-ordinated water molecule and the OH^- group were obtained from Fourier-difference maps. Two of the perchlorate anions are disordered. The site occupancy factors of these disordered oxygen atoms were refined as 0.78 for O(12), O(13) and O(14), 0.22 for O(12′), O(13′) and O(14′), 0.33 for O(21), O(22), O(23) and O(24) and 0.67 for O(21′), O(22′), O(23′) and O(24′), respectively.

All computations were carried out on a PC-586 computer using the SHELXTL-PC program package.[18]

CCDC reference number 186/1294.

See http://www.rsc.org/suppdata/dt/1999/729/ for crystallographic files in .cif format.

Other physical measurements

Absorption spectral measurements were performed on a Shimazu UV-3100 spectrophotometer, ^{1}H NMR spectra on a Bruker AM-500 spectrometer using the residual proton in deuteriated solvent as the internal reference ($CDCl_3$, δ 7.26 or CD_3CN, δ 1.93). Electrospray mass spectra (ES-MS) were recorded on a LCQ system (Finngan MAT, USA) using methanol as mobile phase.. The spray voltage, tube lens offset, capillary voltage and capillary temperature were set at 4.50 kV, 0 V, 17.00 V and 150 °C, respectively, and the quoted *m*/*z* values are for the major peaks in the isotope distribution. Cyclic voltammograms were performed on an EG&G M273 potentiostat/galvanostat system using a platinum disk working electrode (0.008 cm^2), which was polished prior to use and rinsed thoroughly with water and acetone, a platinum wire counter electrode and an Ag–AgCl electrode as reference. All the measurements were carried out at 298 K using purified acetonitrile as solvent and freshly recrystallized 0.1 mol dm^{-3} tetrabutylammonium perchlorate as supporting electrolyte; samples were bubbled with argon prior to each measurement. Ferrocene was added at the end of each experiment as an internal reference. A mercury cathode and a silver wire anode were employed during controlled potential coulometric analysis in the same supporting electrolyte as above. X-Band ESR spectral measurements of complex **2** were carried out on a Bruker 200D-SRC system.

Results and discussion

Structure of $[Cu^I_2L^{56}_2][ClO_4]_2\cdot Et_2O$ 1

Fig. 1 shows the ORTEP[19] representation of the cation structure of $[Cu^I_2L^{56}_2]^{2+}$ with the atom numbering scheme. It is clear from the X-ray structural analysis that the two L^{56} ligands adopt a head-to-tail configuration. Since the ligand is asymmetric two kinds of co-ordination are possible when the ligands interact with homonuclear dimetal ions, one is head-to-head

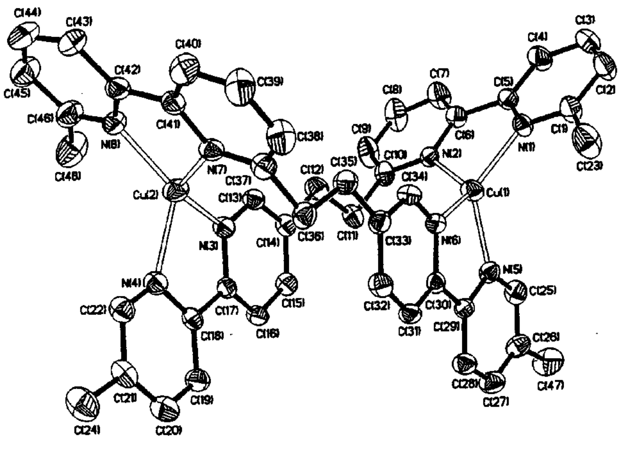

Fig. 1 The structure of the cation $[Cu^I_2L^{56}_2]^{2+}$ with the atom numbering scheme. Thermal ellipsoids are drawn at 50% probability.

(HH) and the other is head-to-tail (HT). However only the head-to-tail species was obtained by reaction of $[Cu(CH_3CN)_4]ClO_4$ with ligand L^{56}. The absence of the head-to-head form is probably due to the steric effect of the terminal methyl and the methylene substituents. The steric control of directional isomerism in helicates of asymmetrically substituted 2,2′ : 6′, 2″ : 6″,2‴-quaterpyridine (qtpy) derivatives has been observed by Constable *et al.*[20] recently, and the appropriate substitution of qtpy at the 4 and 4′ positions leads to the preferred formation of the HH over the HT isomer. Intrinsically, in both their and the current self-assembly systems, the ligand strands in the helicates adopt the arrangement spontaneously to minimize the steric repulsion between the substituents of the pyridine rings. The copper atoms of complex **1** are four-co-ordinated with distorted tetrahedral geometry in which the N–Cu–N bond angles are found in a range from 81.16(12) to 134.04(12)° for Cu(1) and from 81.36(12) to 138.99(13)° for Cu(2), the Cu–N bond lengths are from 1.994(3) to 2.069(3) Å and the mean length of all eight copper–nitrogen bonds is 2.031 Å as listed in Table 2. The N–Cu–N angles and the Cu–N bond lengths of **1** are similar to those of reported complexes such as $[Cu^I_2L^{66}_2]^{2+}$.[3] However, the intermetallic distance of 7.920(2) Å between Cu(1) and Cu(2) for **1** is longer than that of $[Cu^I_2L^{66}_2]^{2+}$ (5.926 Å).[3] This difference is considered to be caused by the different linkage modes of the CH_2CH_2 spacer group to the bipyridine units of the ligands. In the ligand L^{56} the two bipyridines are connected by the CH_2CH_2 spacer group through the 5 and 6′ positions, while the L^{66} ligand consists of two bipyridines bridged by the same spacer group at the 6 and 6′ positions.

Each pyridine ring in complex **1** is planar with atom deviations less than 0.03 Å. The four bipyridine fragments are also almost planar since the dihedral angles between the pyridine groups of each bipyridine subunit are quite small [1/2, 1.94(13); 3/4, 10.83(10); 5/6, 6.19(10)° and 7/8, 0.52(11)°, respectively; the pyridine planes are numbered according to the numbering of the nitrogen atom as shown in Fig. 1]. In the case of complex $[Cu^I_2L^{66}_2]^{2+}$ the planarities of two bipyridine subunits of each ligand are different, the bipyridines containing N(1) and N(2) or N(7) and N(8) being almost planar as reflected by their average dihedral angle of 5°, and the bipyridine subunits with N(3) and N(4) or N(5) and N(6) are twisted about the ring junction with an average angle of 17°.[3] The large deviation from planarity for one of the two bipyridine units in each ligand of the complex $[Cu^I_2L^{66}_2]^{2+}$ has been reported to originate from the steric hindrance induced by the methyl and methylene substituents α to the chelating nitrogens.[3] Such steric hindrance is thought to be much smaller in complex **1** since the methyl and methylene substituents are at the β rather than the α positions to the chelating nitrogens of N(3) and N(4) or N(5) and N(6) in each ligand L^{56}. The decreased strain in **1** is supported by the smaller dihedral angles of N(3) and N(4) or N(5) and N(6) than those of $[Cu^I_2L^{66}_2]^{2+}$ (see above) and by the bending of the terminal pyridine planes involving N(4) and N(5) as reflected by the dihedral angle of 38.3(2)° for $[Cu^I_2L^{66}_2]^{2+}$ and of 16.72(11)° for complex **1**. The results indicate that changing one of the bipyridine connections from the 6 to the 5 position reduces the steric hindrance to formation of a double-stranded helix with Cu^I. Therefore, the ligand L^{56} is beneficial to such formation compared with ligand L^{66}.

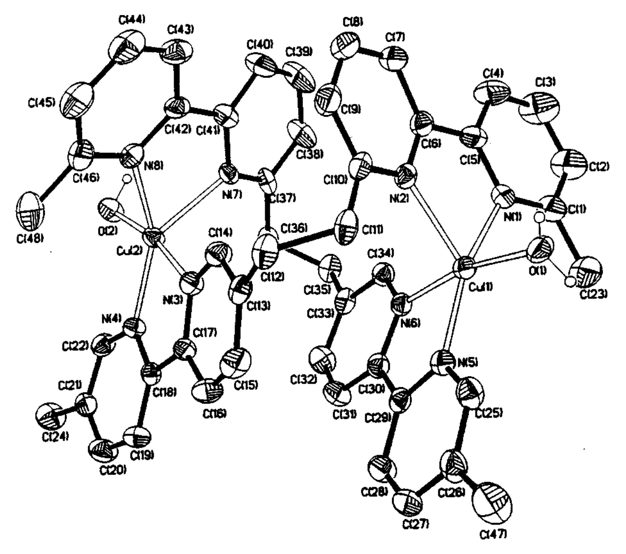

Fig. 2 The structure of the cation $[Cu^{II}_2L^{56}_2(OH)(H_2O)]^{3+}$ with the atom numbering scheme. Thermal ellipsoids are drawn at 50% probability.

As shown in Fig. 1, two ligand strands in **1** intertwine around the copper(I) ions forming a double-stranded helicate, the dihedral angles between two bipyridine units of each ligand being 85.89(7) [between N(1), N(2) and N(3), N(4)] and 82.20(7)° [between N(5), N(6) and N(7), N(8)], respectively. The dihedral angles between the two almost planar bipyridine fragments for Cu(1) [N(1), N(2) and N(5), N(6)] and Cu(2) [N(3), N(4) and N(7), N(8)] are 81.90(6) and 74.60(5)°, respectively. This is in agreement with the distortion from the ideal tetrahedron of each copper site as mentioned above.

Structure of $[Cu^{II}_2L^{56}_2(OH)(H_2O)][ClO_4]_3$ 2

Fig. 2 illustrates the structure of the cation part of $[Cu^{II}_2L^{56}_2(OH)(H_2O)][ClO_4]_3$ **2**. In addition to the two oligobipyridine ligands L^{56}, one H_2O molecule is co-ordinated to Cu(1) and an OH^- group to the Cu(2) atom to form an unsaturated double-stranded dinuclear helical complex. Thus both Cu atoms in **2** are five-co-ordinated with a N_4O donor set. The geometric parameter τ of the polyhedra $Cu(1)N_4O$ and $Cu(2)N_4O$, calculated by using the literature method,[21] are 0.129 and 0.337, respectively. Therefore, the co-ordination geometry of both Cu atoms in **2** can be regarded as a distorted tetragonal pyramid, since the τ value is equal to zero for a perfectly tetragonal geometry while it becomes unity for a perfectly trigonal-bipyramidal geometry, and the larger τ value of the $Cu(2)N_4O$ polyhedron indicates that this is much more distorted than $Cu(1)N_4O$. The atoms O(1), N(1), N(5), N(6) and O(2), N(3), N(4), N(8) form the basal planes of the Cu(1) and Cu(2) sites, respectively, and N(2) and N(7) occupy the corresponding apical positions. The average copper–nitrogen bond length of the basal plane is 2.041 Å for the Cu(1) site and 2.051 Å for the Cu(2) site. The apical bonds are elongated Cu(1)–N(2) 2.208(2) and Cu(2)–N(7) 2.167(2) Å (see Table 2). The deviations of the copper atom from the O(1), N(1), N(5), N(6) and O(2), N(3), N(4), N(8) basal planes are 0.239(1) Å for Cu(1) and 0.372(1) Å for Cu(2), respectively. The metal–metal distance of complex **2** is 6.875(2) Å which is shorter than that of **1**.

Table 1 Crystal data and summary of data collection and structure refinement for complexes **1** and **2**

	$[\mathrm{Cu^I_2L^{56}_2}][\mathrm{ClO_4}]_2\cdot\mathrm{Et_2O}$ **1**	$[\mathrm{Cu^{II}_2L^{56}_2(OH)(H_2O)}][\mathrm{ClO_4}]_3$ **2**
Empirical formula	$C_{52}H_{54}Cl_2Cu_2N_8O_9$	$C_{48}H_{47}Cl_3Cu_2N_8O_{14}$
M	1133.01	1193.37
T/K	293(2)	293(2)
Crystal system	Triclinic	Monoclinic
Space group	$P\bar{1}$	$P2_1/n$
a/Å	11.2999(7)	11.216(3)
b/Å	14.669(2)	21.616(4)
c/Å	18.003(2)	20.795(5)
α/°	113.605(9)	
β/°	95.520(10)	95.91(2)
γ/°	103.020(7)	
U/Å^3, Z	2605.4(5), 2	5015(2), 4
μ/mm^{-1}	0.982	1.084
No. reflections measured	10307	22769
No. unique reflections	8844[R(int) = 0.0884]	8368[R(int) = 0.0517]
Variables	686	742
Goodness of fit indicator	1.046	1.064
$R1$	0.0588	0.0712
$wR2$ (*all data*)	0.1528, (0.1867)	0.1319, (0.1522)

Table 2 Selected bond lengths (Å) and angles (°) for complexes **1** and **2**

	$[\mathrm{Cu^I_2L^{56}_2}]$-$[\mathrm{ClO_4}]_2\cdot\mathrm{Et_2O}$ **1**	$[\mathrm{Cu^{II}_2L^{56}_2(OH)}$-$\mathrm{(H_2O)}][\mathrm{ClO_4}]_3$ **2**
Cu(1)–N(1)	2.004(3)	2.066(2)
Cu(1)–N(2)	2.057(3)	2.208(2)
Cu(1)–N(5)	2.052(3)	2.018(2)
Cu(1)–N(6)	2.012(3)	2.039(2)
Cu(2)–N(3)	1.994(3)	2.028(2)
Cu(2)–N(4)	2.069(3)	2.011(2)
Cu(2)–N(7)	2.061(3)	2.167(2)
Cu(2)–N(8)	2.001(3)	2.113(2)
Mean of Cu–N	2.031	2.081
Cu(1)–O(1)		1.909(2)
Cu(2)–O(2)		1.912(2)
N(1)–Cu(1)–N(2)	81.86(11)	77.46(7)
N(1)–Cu(1)–N(5)	126.54(12)	160.28(7)
N(1)–Cu(1)–N(6)	134.04(12)	92.91(7)
N(2)–Cu(1)–N(5)	113.87(12)	121.66(7)
N(2)–Cu(1)–N(6)	123.43(11)	98.57(7)
N(5)–Cu(1)–N(6)	81.16(12)	80.14(7)
O(1)–Cu(1)–N(1)		92.39(7)
O(1)–Cu(1)–N(2)		93.05(7)
O(1)–Cu(1)–N(5)		91.36(7)
O(1)–Cu(1)–N(6)		168.03(7)
N(3)–Cu(2)–N(4)	81.36(12)	80.16(7)
N(3)–Cu(2)–N(7)	125.01(11)	99.53(7)
N(3)–Cu(2)–N(8)	138.99(13)	89.39(7)
N(4)–Cu(2)–N(7)	107.31(12)	134.69(7)
N(4)–Cu(2)–N(8)	123.07(12)	147.48(7)
N(7)–Cu(2)–N(8)	81.99(12)	77.23(7)
O(2)–Cu(2)–N(3)		170.11(7)
O(2)–Cu(2)–N(4)		91.31(7)
O(2)–Cu(2)–N(7)		90.01(7)
O(2)–Cu(2)–N(8)		95.30(7)

All atoms of each pyridine ring in **2** are also planar and the two pyridine rings of the bipyridine units with N(1), N(2); N(3), N(4) and N(5), N(6) are almost coplanar since the dihedral angles are quite small [1/2, 8.43(8); 3/4, 9.47(7) and 5/6, 1.74(7)°], while the bipyridine unit with N(7) and N(8) shows a large deviation in planarity [dihedral angle 7/8, 17.84(9)°]. The helication of each ligand L^{56} of **2** is confirmed by the dihedral angles of 80.47(3)° between bipyridine fragments with N(1), N(2) and N(3), N(4) and 83.84(3)° between two bipyridine units with N(5), N(6) and N(7), N(8).

Each ligand L^{56} has two bipyridine units, one is 5,5′-disubstituted and another is 6,6′-disubstituted. As shown in Fig. 2, a 5,5′-disubstituted bipyridine of one ligand and a 6,6′-disubstituted bipyridine of another ligand co-ordinate to the same copper(II) ion, *i.e.* the two ligand strands are arranged in head-to-tail configuration in complex **2**. Such an arrangement reduces the steric hindrance between the methyl and the methylene substituents and makes possible the formation of the dinuclear copper(II) double-stranded helicate. In the case of ligand L^{66}, the two bipyridines are both 6,6′-disubstituted, there is steric hindrance between the methyl and methylene substituents α to the chelating nitrogens and such a steric effect is considered to inhibit the formation of helicate complexes of L^{66} with Cu^{II}.[3] The distances between the two terminal methyls C(1)···C(25) and C(24)···C(48) of $[\mathrm{Cu^I_2L^{66}_2}]^{2+}$ are 4.57 and 4.81 Å, and the separations between the methylene substituents C(12)···C(36) and C(13)···C(37) are 4.48 and 5.51 Å, respectively. The corresponding distances are 7.002(8) [C(23)···C(47)], 7.235(7) [C(24)···C(48)], 6.082(8) [C(11)···C(35)] and 6.104(8) Å [C(12)···C(36)] for **1** and 7.220(10) [C(23)···C(47)], 6.736(13) [C(24)···C(48)], 7.318(12) [C(11)···C(35)] and 7.307(10) Å [C(12)···C(36)] for **2**. It is obvious that the distances between the two terminal methyls or the methylene substituents in **1** and **2** are longer than those of $[\mathrm{Cu^I_2L^{66}_2}]^{2+}$. On the other hand, the three nitrogen atoms in the basal plane of the Cu(1) site of **2** are N(5) and N(6) from the 5,5′-disubstituted bipyridine unit and N(1) from the 6,6′-disubstituted bipyridine unit, while the other nitrogen atom N(2) of the 6,6′-disubstituted bipyridine unit occupies the apical position of the distorted square pyramid. A similar situation was observed for the Cu(2) site. The co-ordination of the 6,6′-disubstituted bipyridine unit out of the basal plane probably contributes to the differing planarities of the bipyridine groups as mentioned above. These arrangements were considered to reduce the steric hindrance of the methyl and methylene substituents in the complex **2**.

The present study demonstrates that the ligand L^{66} strongly stabilizes the copper(I) *versus* copper(II) complex due to the steric hindrance of the methyl and methylene substituents α to the chelating nitrogens, which inhibit the formation of a distorted tetragonal pyramidal copper(II) complex as proposed by Lehn and co-workers.[3] The results indicate that the change of the linkage mode between bipyridine units in ligand L^{56} makes it possible to co-ordinate Cu^{II} to form a double helicate which is not obtained using the ligand L^{66}.

An intermolecular hydrogen bond is formed between the OH$^-$ group in one cation and a H$_2$O molecule in a neighboring cation. The O(1)···O(2A) separation is 2.403(2) Å, and the O(1)–H(1A)···O(2A) angle is 158.4(2)°; symmetry code A $-0.5 + x, 0.5 - x, 0.5 + z$.

Electrospray mass spectra

The ES mass spectrum of complex **1** includes three main peaks,

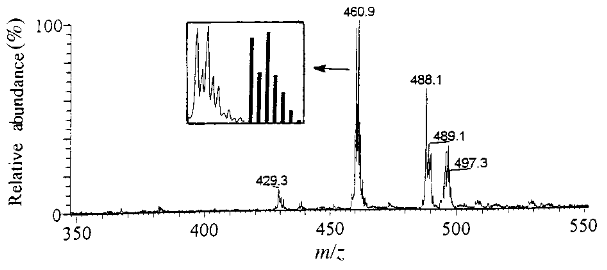

Fig. 3 Electrospray mass spectrum of $[Cu^{II}_2L^{56}_2(OH)(H_2O)][ClO_4]_3$ **2** in acetonitrile; the inset shows the observed (traces) and calculated (bars) isotopic distributions for the major peak at *m*/*z* 460.9.

at *m*/*z* 430.3 corresponding to the most abundant ion $[Cu^I_2L^{56}_2]^{2+}$, a small peak at *m*/*z* 958.9 resulting from $\{[Cu^I_2L^{56}_2](ClO_4)\}^+$ and a small peak at *m*/*z* 795.0 corresponding to the $[Cu^IL^{56}_2]^+$ cation. There are four main peaks observed in the ES mass spectrum of **2** as shown in Fig. 3, a major peak at *m*/*z* = 460.9 corresponding to $\{[Cu^I_2L^{56}_2](CH_3OH)_2\}^{2+}$, the peaks at *m*/*z* 488.1, 497.3 and 429.3 corresponding to $\{[Cu^{II}_2L^{56}_2(OH)](ClO_4)\}^{2+}$, $\{[Cu^{II}_2L^{56}_2(OH)(H_2O)](ClO_4)\}^{2+}$ and $[Cu^I_2L^{56}_2]^{2+}$, respectively. The appearances of $\{[Cu^I_2L^{56}_2](CH_3OH)_2\}^{2+}$ and $[Cu^I_2L^{56}_2]^{2+}$ indicate that the majority of the Cu^{II} was reduced to Cu^I under the electrospray condition. When the capillary temperature was set as 200 °C the relative intensity of the peaks at *m*/*z* 488.1 and 497.3 decreased to almost zero, the cation at *m*/*z* 429.3 becoming the major species. The inset compares observed and calculated isotope distributions for the major peak at *m*/*z* = 460.9; the agreement is excellent and ensured our assignments.

Electrochemistry and UV-visible spectra of complexes 1 and 2

The electrochemical properties of complexes **1** and **2** were investigated by cyclic voltammetry. Complex **1** showed a quasi-reversible wave, at $E_{\frac{1}{2}} = +0.77$ V ($\Delta E_p = 70$ mV, $i_{pc}/i_{pa} = 0.69$) *vs.* Ag–AgCl in CH_3CN at scan rate 100 mV s^{-1}. The $E_{\frac{1}{2}}$ value is similar to those of the reported analog $[Cu^I_2L^{66}_2]^{2+}$ ($E_{\frac{1}{2}} = +0.88$ V *vs.* SCE) and $[Cu(dmbpy)_2]^+$ ($E_{\frac{1}{2}} = +0.72$ V *vs.* SCE; dmbpy = 6,6′-dimethyl-2,2′-bipyridine).[3] Complex **2** exhibited a quasi-reversible wave at $E_{\frac{1}{2}} = +0.64$ V ($\Delta E_p = 80$ mV, $i_{pc}/i_{pa} = 0.89$) *vs.* Ag–AgCl in CH_3CN solution at scan rate 400 mV s^{-1}, however the redox waves became irreversible at scan rates of 100, 50, and 20 mV s^{-1}. The $E_{\frac{1}{2}}$ value is similar to that of complex **1** and higher than that of the reported mononuclear copper(II) complex $[CuL'(H_2O)]^{2+}$ ($E_{\frac{1}{2}} = +0.19$ V *vs.* SCE) in which the Cu^{II} has a distorted trigonal bipyramidal geometry [where L′ = 1,2-bis(9-methyl-1,10-phenanthrolin-2-yl)ethane].[22] Such a significant difference of $E_{\frac{1}{2}}$ values between complex **2** and $[CuL'(H_2O)]^{2+}$ is considered to be due to the different co-ordination environments and geometry. Controlled potential coulometric analysis showed two-electron processes for both complexes **1** and **2**.

The UV-visible spectra of complexes **1** and **2** in acetonitrile solution were measured at room temperature. Complex **1** shows a transition near $\lambda_{max} = 444$ nm ($\varepsilon = 5976$ M^{-1} cm^{-1}) which can be assigned to metal-to-ligand charge-transfer (MLCT) according to the literature.[5a,e,16] The appearance of absorption at about $\lambda_{max} = 629$ nm ($\varepsilon = 2600$ M^{-1} cm^{-1}) for **2** arises from d_{xz}, $d_{yz} \longrightarrow d_{x^2-y^2}$ transitions. The high-energy transitions located in the UV region of both **1** (303 nm, 73570 M^{-1} cm^{-1}; 253 nm, 66770 M^{-1} cm^{-1}) and **2** (317 nm, 62080 M^{-1} cm^{-1}; 251 nm, 53570 M^{-1} cm^{-1}) are from intraligand $\pi \longrightarrow \pi^*$ transitions.

^{1}H NMR Spectra of complex 1 and electron spin resonance spectra of 2

The ^{1}H NMR spectra of the ligand L^{56} in CD_3CN and complex **1** in acetonitrile-d$_3$ at 298 K are shown in Fig, 4. Only one kind of ligand proton signal was observed for **1** within the NMR timescale, although there is no C_2 symmetry axis or center for **1** in the solid state. For resolving all the protons of **1**, COSY and NOSY experiments were employed, and peak attributions of the aromatic proton are as shown in Fig. 4(b). The chemical shifts of the aromatic proton in the complex are different from those of free L^{56}. For example, the proton e shifts upfield by more than 0.4 ppm, while b shifts downfield by only 0.15 ppm, indicating that e lies in the shielding region of the bipyridine subunits of the second ligand which is similar to the reported case of $[Cu^I_2L^{66}_2]^{2+}$.[3]

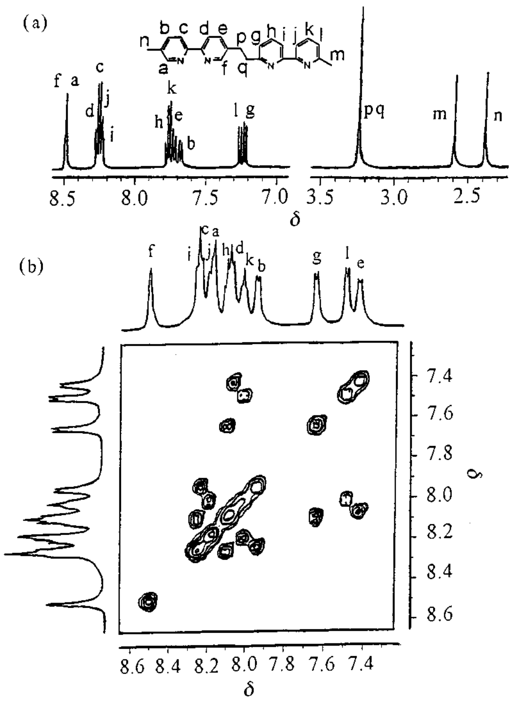

Fig. 4 (a) The 500 MHz ^{1}H NMR spectra of ligand L^{56} in CDCN. (b) The COSY spectrum of $[Cu^I_2L^{56}_2][ClO_4]_2$ **1** in CD_3CN at 298 K.

The *g* values of the ESR spectra in a polycrystalline powder and in an acetonitrile-1,4-dioxane (50 : 50 v/v) solution of complex **2** at room temperature are 2.060 and 2.072, respectively. The spectrum in acetonitrile-1,4-dioxane (50 : 50 v/v) solution at 100 K, gave $g_{\parallel} = 2.244$, $g_{\perp} = 2.063$ and $A_{\parallel} = 160$ G.

Conclusion

The present results show that the ligand containing two bipyridine units linked by a CH_2CH_2 bridge at the 5,6′ positions is able to form double-stranded helical complexes with copper(I) and copper(II) ions. This was confirmed by X-ray structural analysis and ES-MS spectra. The structure in solution of **1** was investigated by ^{1}H NMR spectroscopy.

The copper(II) complex **2** is thought to be the first example of a double-stranded helical structure which contains two di-substituted bipyridine units co-ordinating to the same copper(II) ions. It is clear from our study that the self-assembly of inorganic helicates containing bipyridine units bridged by a CH_2CH_2 group is partially controlled by the linkage mode between the bipyridine units, the co-ordination geometries of the metal ions and the flexibility of the spacer groups. The change of the linkage mode between the bipyridine units in ligand L^{56} makes it possible to co-ordinate Cu^{II} to form a double helicate which was not obtained using the ligands L^{55} and L^{66}.

Acknowledgements

This work is supported by the National Nature Science Foundation of China.

References

1 F. Vögtle, *Supramolecular Chemistry*, Wiley, Chichester, 1993; J.-M. Lehn, *Supramolecular Chemistry: Concept and Perspectives*, VCH, Weinheim, 1995.

2 E. C. Constable, *Prog. Inorg. Chem.*, 1994, **42**, 67.

3 M.-T. Youinou, R. Ziessel and J.-M. Lehn, *Inorg. Chem.*, 1991, **30**, 2144.

4 E. C. Constable, *Tetrahedron*, 1992, **48**, 10013; C. Piguet, G. Bernardinelli and G. Hopfgartner, *Chem. Rev.*, 1997, **97**, 2005.

5 (*a*) J.-M. Lehn, A. Rigault, J. Siegel, J. Harrowfield, B. Chevrier and D. Morras, *Proc. Natl. Acad. Sci. U.S.A.*, 1987, **84**, 2565; (*b*) U. Koert, M. M. Harding and J.-M. Lehn, *Nature*, 1990, **346**, 339; (*c*) A. Pfeil and J.-M. Lehn, *J. Chem. Soc.*, *Chem. Commun.*, 1992, 838; (*d*) C. R. Woods, M. Benaglia, F. Cozzi and J. S. Seigel, *Angew. Chem.*, *Int. Ed. Engl.*, 1996, **35**, 1830; (*e*) A. Rigault and J.-M. Lehn, *Angew. Chem.*, *Int. Ed. Engl.*, 1988, **27**, 1095.

6 Y. Fu, J. Sun, Q. Li, Y. Chen, W. Dai, D. Wang, T. C. W. Mak, W. Tang and H. Hu, *J. Chem. Soc.*, *Dalton Trans.*, 1996, 2309.

7 T. M. Garrett, U. Koert, J.-M. Lehn, A. Rigault, D. Meyer and J. Fischer, *J. Chem. Soc.*, *Chem. Commun.*, 1990, 557.

8 K. T. Potts, M. Keshavarz-K, F. S. Tham, H. D. Abtuna and C. Arana, *Inorg. Chem.*, 1993, **32**, 4422, 4436.

9 R. Krämer, J.-M. Lehn, A. DeCian and J. Fischer, *Angew. Chem.*, *Int. Ed. Engl.*, 1993, **32**, 703.

10 G. Bernardinelli, C. Piguet and A. F. Williams, *Angew. Chem.*, *Int. Ed. Engl.*, 1992, **31**, 1621; C. Piguet, G. Bernardinelli, B. Bocquet, O. Schaad and A. F. Williams, *Inorg. Chem.*, 1994, **33**, 4112; C. Piguet, J.-C. G. Bünzli, G. Bernardinelli, G. Hopfgartner, S. Petoud and O. Schaad, *J. Am. Chem. Soc.*, 1996, **118**, 6681; C. Piguet, E. Rivara-Minten, G. Bernardinelli, J.-C. G. Bünzli and G. Hopfgartner, *J. Chem. Soc.*, *Dalton Trans.*, 1997, 421.

11 B. Hasenknopf, J.-M. Lehn, N. Boumediene, A. Dupont-G, A. V. Dorsselaer, B. Kneisel and D. Fenske, *J. Am. Chem. Soc.*, 1997, **119**, 10956.

12 B. Hasenknopf, J.-M. Lehn, B. O. Kneisel, G. Baum and D. Fenske, *Angew. Chem.*, *Int. Ed. Engl.*, 1996, **35**, 1838.

13 G. R. Newkome, W. E. Puckett, G. E. Kiefer, V. K. Gupta, Y. Xia, M. Coreil and M. A. Hackney, *J. Org. Chem.*, 1982, **47**, 4116.

14 W. H. F. Sasse and C. P. Whittl, *J. Chem. Soc.*, 1961, 1347; G. M. Badger and W. H. F. Sasse, *J . Chem. Soc.*, 1956, 616.

15 B. J. Hathaway, D. G. Holah and J. D. Postlethwaite, *J. Chem. Soc.*, 1961, 3215.

16 J.-C. Rodriguez-U, B. Alpha, D. Plancherel and J.-M. Lehn, *Helv. Chim. Acta*, 1984, **67**, 2264.

17 XSCANS, Version 2.1, Siemens Analytical X-ray Instruments, Inc., Madison, WI, 1994.

18 Siemens, SHELXTL, Version 5.0, Siemens Industrial Automation, Inc. Analytical Instrumentation, Madison, WI, 1995.

19 C. K. Johnson, ORTEP, Report ORNL-5138, Oak Ridge National Laboratory, Oak Ridge, TN, 1976.

20 E. C. Constable, F. Heirtzler, M. Neuburger and M. Zehnder, *J. Am. Chem. Soc.*, 1997, **119**, 5606.

21 A. W. Addison, T. N. Rao, J. Reedijk, J. V. Rijn and G. C. Verschoor, *J. Chem. Soc.*, *Dalton Trans.*, 1984, 1349.

22 Y. Yao, M. W. Perkovic, D. P. Rillema and C. Woods, *Inorg. Chem.*, 1992, **31**, 3956.

Paper 8/08550A